that in the solid state, the axial coordination sites about the metal ion are partly occupied by atoms of neighboring molecules.

For $[Cu\text{-}Zn(F_6acac)_3^-]$ a dynamic Jahn-Teller behavior is observed. At 115°K a spectrum, Figure 3, typical of a tetragonally elongated octahedron is observed. A continuous variation from the low-temperature spectrum to a nearly isotropic spectrum with $g = 2.177 = {}^1/_3(g_\parallel + 2g_\perp)$ at about 350°K is seen.

The temperature dependence of the epr spectrum for $[Cu\text{-}Zn(F_6acac)_3^-]$ suggests that the complex oscillates or pseudorotates between three tetragonally distorted configurations. An isotropic g value is observed at about the same temperature for copper(II)-doped tris(phenanthroline)zinc(II) nitrate dihydrate.[34] Thus it is reasonable to assume that similar energy barriers separate the three possible configurations in both of these tris chelates. In contrast, $Cu\text{-}Zn(F_6acac)_2(py)_2$ shows an anisotropic spectrum to 370°K and appears far from reaching isotropic behavior (a result of a relatively high energy barrier). The crystallographic data indicate a smaller tetragonality value for the pyridine adduct than for the CuO_6 complex.[35] However, the *cis*-CuO_4N_2 species cannot, by symmetry, become isotropic (as is possible for CuO_6 or CuN_6 complexes).

Acknowledgments. This work was supported by the National Science Foundation, Grant GP-11701. Thanks are extended by J. P-S. to the Lubrizol Foundation for an A. W. Smith Fellowship and to the Colombian Institute "ICFES" for financial support.

Registry No. $Zn(F_6acac)_2(py)_2$, 38402-93-6; $Cu(F_6acac)_2bipy$, 29868-71-1; $Zn(F_6acac)_2bipy$, 42087-49-0; $Cu(F_6acac)_2(py)_2$, 38496-50-3; $Zn(F_6acac)_3^-$, 42087-51-4; $Zn(F_6acac)_2(H_2O)_2$, 42087-52-5; $Zn(F_6acac)_2$, 14949-70-3; $Cu(F_6acac)_2$, 14781-45-4; $Zn(F_6acac)_2(H_2O)$, 42087-53-6; Cu, 7440-50-8.

(34) G. F. Kokoszka, C. W. Reinmann, H. C. Allen, and G. Gordon, *Inorg. Chem.*, 6, 165 (1967).

(35) P. T. Miller, P. G. Lenhert, and M. D. Joestin, *Inorg. Chem.*, 12, 218 (1973), recently stated that "most literature reports on distortions in six-coordinate Cu(II) complexes are incorrect in attributing these distortions to the Jahn-Teller effect." This comment, although fundamentally correct, is misleading. The Jahn-Teller theorem, loosely stated, requires that the lowest energy electronic configuration in a nonlinear molecule be nondegenerate. However, the energy difference between the hypothetically undistorted molecule with orbital degeneracy and the distorted species in its equilibrium geometry is the point of interest. This energy difference will depend on several factors, some of which are only poorly understood at present. Clearly metal-ligand bonding parameters are involved and must be taken into account (see T. S. Davis, J. P. Fackler, and M. J. Weeks, *Inorg. Chem.*, 7, 1994 (1968)). These appear to be fairly constant for similar ligands. In the solid state, various intermolecular forces also play an important role in stabilizing the equilibrium geometry. This is shown in our work[2] on $Zn\text{-}Cu(F_6acac)_2(py)_2$ where, strictly speaking, the Jahn-Teller theorem is not applicable. It is also apparent from the structural and epr studies on $Cu(F_6acac)_3^-$, a $Cu^{II}O_6$ species with significantly different Cu-O bond lengths.[22] The important consideration is that a large Jahn-Teller distortion force (A. D. Liehr, *Progr. Inorg. Chem.*, 3, 281 (1962)), which produces a significant electronic splitting of the E ground state, requires that the minimum in the potential surface occurs at a fairly large value of the vibration coordinate q (of the order of 0.16 Å) for normal (2×10^5 dyn/cm) metal-ligand force constants. The crystallographic detectability of this distortion, however, will depend on whether the crystal forces present are large enough in a given system to prevent pseudorotation. It is the barrier to pseudorotation which appears to be small in most ML_6 complexes—not the Jahn-Teller distorting force.

Contribution from the Department of Chemistry, University of California, Riverside, California 92502

Paramagnetic Resonance Investigation of $Au[1,2\text{-}S_2C_2(CN)_2]_2^{2-}$, a Formal Gold(II) Complex

RONALD L. SCHLUPP and AUGUST H. MAKI*

Received May 16, 1973

Electron paramagnetic resonance spectra of the square-planar complex $Au[S_4C_4(CN)_4]^{2-}$ have been obtained over a range of temperature in magnetically dilute single crystals of $Ni[S_4C_4(CN)_4][(n\text{-}Bu)_4N]_2 \cdot 2CH_3CN$ and $M[S_4C_4(CN)_4][(n\text{-}Bu)_4N]$ (M = Ni, Pd, Pt). In the former host the principal axes of **g** and **P** are coincident with the molecular axes while in the latter hosts only the axes of **P** are coincident with the molecular axes, the **g** axes being rotated ~8.5° at a temperature of 22°. The parameters are found to be temperature dependent including the angle of noncoincidence; g_{zz} increases markedly with increasing temperature. The results are shown to be consistent with a ground-state hole configuration $(B_{1g})^2(A_g)^1$ where A_g is primarily a ligand-based orbital with ~15% 6s and smaller 5d admixtures and B_{1g} is the normally half-filled antibonding orbital in square-planar d^9 complexes. The rotation of **g** is explained in terms of a reduction of the site symmetry. The temperature dependences are ascribed to the vibronic mixing of the excited configuration $(A_g)^2(B_{1g})^1$. Asymmetries in the spectra allowed the determination of the relative signs of A_{iso} and P_{zz} (opposite) and the absolute sign of the nuclear g value (positive).

Introduction

Although complexes in which gold is present in a 2+ formal oxidation state are of great interest because of their possible electronic similarity with Cu(II) complexes, very few have been reported in the literature. Bis(diethyldithiocarbamato)gold(II) was synthesized by Vanngard and Akerstrom,[1] who did not isolate the complex but did observe its solution epr spectrum which showed a characteristic four-line hyperfine pattern expected for ^{197}Au ($I = {}^3/_2$). van Willigen and van Rens[2] were able to incorporate the Au(II) complex into a single crystal of the diamagnetic Ni(II) complex and obtain epr spectra of an oriented magnetically dilute sample. The spectra showed the anomalous feature of having weak satellites outside of the main four-line pattern which was unequally spaced. In contrast to this is the normal situation in which the satellites lie within an approxi-

(1) T. Vanngard and S. Akerstrom, *Nature (London)*, 184, 183 (1959).

(2) H. van Willigen and J. G. M. van Rens, *Chem. Phys. Lett.*, 2, 283 (1968).

mately equally spaced hyperfine pattern.[3] These spectra were interpreted in terms of a spin Hamiltonian in which the magnitudes of the ^{197}Au hyperfine and quadrupole interactions were comparable. This unusual situation arises because of the rather small magnetic moment of ^{197}Au relative to its large quadrupole moment.

A report of a gold(II)-phthalocyanine complex has appeared,[4] but this complex was not isolated nor was its epr spectrum completely characterized. Warren and Hawthorne[5] have reported a formally gold(II) dicarbollide complex, $[\pi\text{-}(3)\text{-}1,2\text{-}B_9C_2H_{11}]_2Au^{2-}$, which has $\mu_{eff} = 1.79$ BM, consistent with an $S = 1/2$ ion but the epr of this complex was not reported.

A tetraalkylammonium salt of bis(maleonitriledithiolato)-gold(II), $Au(mnt)_2^{2-}$, was characterized by Waters and Gray,[6] who reported its solution epr spectrum. An epr investigation of a magnetically dilute single crystal containing this complex by van Rens and deBoer[7] revealed anomalous behavior of the hyperfine structure similar to that observed in the dithiocarbamate complex.

We present here a detailed epr study of the complex bis-(maleonitriledithiolato)gold(II) which we have investigated in several host crystals and over a range of temperature. Our conclusion from these measurements is that upon reduction of the Au(III) complex, the electron enters an orbital which is largely a ligand-based orbital of A_g symmetry (in D_{2h}). The metal character of this orbital is principally 6s containing a small amount of 5d-orbital character due to mixing under the A_g representation ($5d_{z^2}$ and $5d_{x^2-y^2}$ in the axis system of Figure 1), by low-symmetry crystal fields ($5d_{xz}$) and by temperature-dependent vibronic coupling ($5d_{xy}$). The antibonding B_{1g}* orbital which is half-filled in square-planar Cu(II) complexes is not occupied in the Au(II) complex. These conclusions explain the large temperature dependence of the g tensor, of the isotropic hyperfine coupling, and of the quadrupole tensor as well as the deviation of the principal axis system of the g tensor from that of the quadrupole tensor and its temperature dependence. From asymmetries in the principal axes spectra we are able to determine that the sign of the principal quadrupole tensor value P_{zz} (expected to be negative) is opposite to that of the nearly isotropic principal hyperfine values and that the absolute sign of the ^{197}Au nuclear g value is positive.

Experimental Section

The compounds $Au(mnt)_2(tba)$ [$tba^+ = (n\text{-}C_4H_9)_4N^+$], $Cu(mnt)_2(tba)_2$, $Rh(mnt)_2(tba)_2$, $Ni(mnt)_2(tba)_2$, $Pd(mnt)_2(tba)_2$, and $Pt(mnt)_2(tba)_2$ were prepared by the published methods.[8-11] Single crystals of $M(mnt)_2(tba)_2$ (M = Ni, Pd, Pt) doped with $Au(mnt)_2(tba)_2$ were grown from saturated, degassed acetone solutions of the diamagnetic host containing $Au(mnt)_2(tba)$ and sodium amalgam. Single crystals of doped $Ni(mnt)_2(tba)_2 \cdot 2CH_3CN$ were prepared by a similar procedure using CH_3CN (acetonitrile) as solvent. Since the structure of the CH_3CN-containing crystal is not known, $Cu(mnt)_2^{2-}$ and $Rh(mnt)_2^{2-}$ were also present in solution and entered the crystals substitutionally. The epr signals of these ions, which have been studied[12] in crystals of known structure, served to locate the principal molecular axes of the host crystal. The crystals of doped $Ni(mnt)_2(tba)_2 \cdot 2CH_3CN$ were unstable in air, rapidly losing solvent. They could be stored indefinitely in an atmosphere saturated with CH_3CN. Epr measurements were made with the single crystal in contact with solvent. The stoichiometry of the CH_3CN-containing crystal was established from weight loss measurements at 120°.

Unit cell parameters and crystal morphology for $Ni(mnt)_2(tba)_2$, $Pd(mnt)_2(tba)_2$, and $Pt(mnt)_2(tba)_2$ were obtained by standard X-ray diffraction and optical goniometry techniques. The crystals were mounted on plastic wedges whose face angles were calculated from the crystal structure of the isomorphous cobalt complex[13] so that the magnetic field in the epr measurements could be rotated in a molecular plane. The molecular axes system is shown in Figure 1.

Epr measurements were made at a microwave frequency of 9.5 GHz on a Varian V-4502 spectrometer using a V-3800 15-in. magnet equipped with a Mark II Fieldial. The microwave frequency was measured with a Hewlett-Packard Model 2590A frequency converter and Model 5245L frequency counter. Magnetic field measurements were made with a proton gaussmeter and the same frequency counter. Variable-temperature measurements were made with a Varian V-4535 "Bigstack" cavity with a cylindrical polyurethane foam dewar which passed through it. The temperature was controlled with a Varian V-4540 variable-temperature apparatus using nitrogen gas flow and measured with a copper–constantan thermocouple attached to a Leeds and Northrup Model 8692 temperature potentiometer.

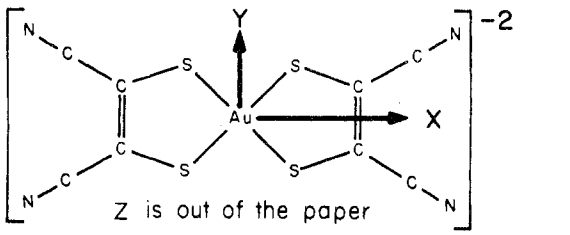

Figure 1. Molecular coordinate system for $Au(mnt)_2^{2-}$.

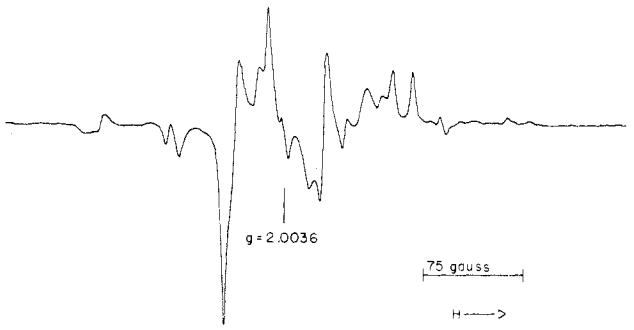

Figure 2. X-Band epr spectrum of $Au(mnt)_2^{2-}$ at −170° in 4:1 dimethylformamide–chloroform.

Results

Cyclic voltammetry[14] of $Au(mnt)_2^-$ in dimethyl sulfoxide showed a reversible couple with cathodic and anodic peaks at −0.46 and −0.35 V *vs.* sce. Constant-potential coulometry near the peak potentials revealed the reduction to be a one-electron reversible process. Room-temperature epr of the dianion in acetonitrile or acetone solution yielded identical four-line spectra with $g_{iso} = 2.0030$ and $a(^{197}Au) = 42.3 \times 10^{-4}$ cm^{-1}. The X-band epr spectrum of a 4:1 dimethylformamide-chloroform glass of the dianion at −170° is shown in Figure 2. Because of its complexity no attempt was made to interpret it.

(3) B. Bleaney, *Phil. Mag.*, 42, 441 (1951).
(4) A. MacCragh and W. S. Koski, *J. Amer. Chem. Soc.*, 87, 2496 (1965).
(5) L. F. Warren, Jr., and M. F. Hawthorne, *J. Amer. Chem. Soc.*, 90, 4823 (1968).
(6) J. H. Waters and H. B. Gray, *J. Amer. Chem. Soc.*, 87, 3534 (1965).
(7) J. G. M. van Rens and E. de Boer, *Mol. Phys.*, 19, 745 (1970).
(8) A. Davison, N. Edelstein, R. H. Holm, and A. H. Maki, *Inorg. Chem.*, 2, 1227 (1963).
(9) H. B. Gray, R. Williams, I. Bernal, and E. Billig, *J. Amer. Chem. Soc.*, 84, 3596 (1962).
(10) E. Billig, R. Williams, I. Bernal, J. H. Waters, and H. B. Gray, *Inorg. Chem.*, 3, 663 (1964).
(11) E. Billig, S. I. Shupack, J. H. Waters, R. Williams, and H. B. Gray, *J. Amer. Chem. Soc.*, 86, 926 (1964).
(12) A. H. Maki, N. Edelstein, A. Davison, and R. H. Holm, *J. Amer. Chem. Soc.*, 86, 4580 (1964).
(13) J. D. Forrester, A. Zalkin, and D. H. Templeton, *Inorg. Chem.*, 3, 1500 (1964).
(14) The apparatus used was similar to that described by F. Lalor, M. F. Hawthorne, A. H. Maki, K. Darlington, A. Davison, H. B. Gray, Z. Dori, and E. I. Stiefel, *J. Amer. Chem. Soc.*, 89, 2278 (1967).

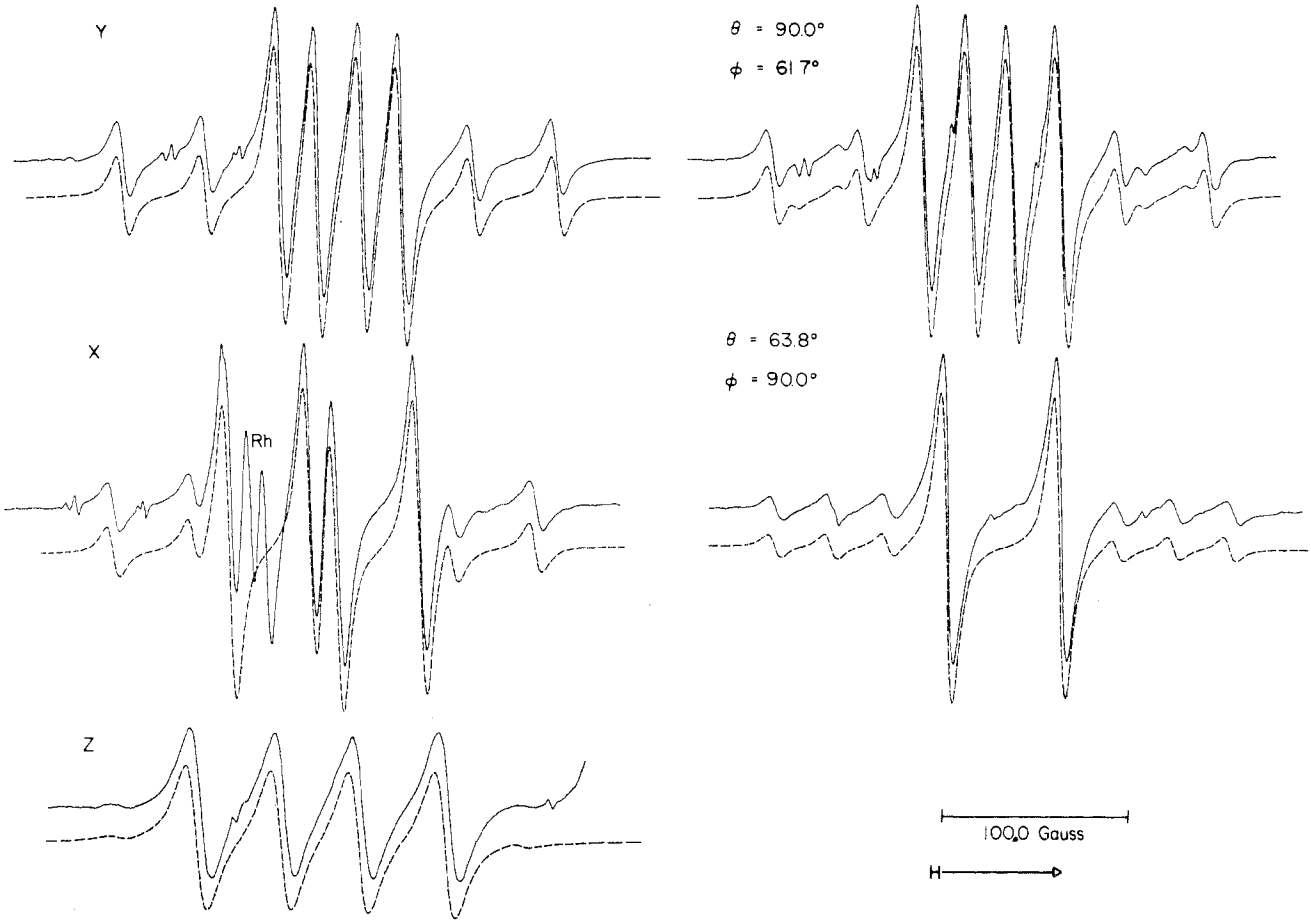

Figure 3. Room-temperature measured (solid lines) and calculated (dashed lines) X-band epr spectra of $Au(mnt)_2^{2-}$ doped into $Ni(mnt)_2(tba)_2 \cdot 2CH_3CN$. Spectra were recorded along the indicated molecular axes and in the *xy* and *yz* planes. θ and ϕ are the usual polar angles. The narrow doublet lines not reproduced in the calculated spectra are from $Cu(mnt)_2^{2-}$ ($^{63,65}Cu$), and the Rh-labeled doublet is from $Rh(mnt)_2^{2-}$.

Qualitatively, the epr spectra of $Au(mnt)_2^{2-}$ in single crystals of $Ni(mnt)_2(tba)_2$ and $Ni(mnt)_2(tba)_2 \cdot 2CH_3CN$ are similar. With the magnetic field, **H**, along a molecular axis, the spectrum is composed of a quartet of unequally spaced intense lines flanked on each side by a pair of weaker lines. As **H** is rotated away from a principal molecular axis in a molecular plane, an additional pair of weak lines gradually appears near the pairs of satellites. With **H** at specific angles in the *xz* or *yz* molecular planes, the quartet of strong lines coalesce into two strong lines, while the four satellite lines on each flank collapse into three lines. The solid curves in Figure 3 show the room-temperature epr signals of $Au(mnt)_2^{2-}$ in the $Ni(mnt)_2(tba)_2 \cdot 2CH_3CN$ host with **H** along the three principal molecular axes as well as two intermediate orientations in the *xy* and *yz* molecular planes. Since the structure of this host is not known, the crystal was oriented using the epr signals of $Cu(mnt)_2^{2-}$ and $Rh(mnt)_2^{2-}$ whose magnetic principal axes are known to coincide with the symmetry axes of the molecule.[12] The dashed curves are calculated using the solutions of the spin hamiltonian to be discussed below.

In each host crystal studied, the experimental line positions and intensities were given within the experimental error in any measured orientation of **H** by the spin hamiltonian

$$\mathcal{H} = \beta \mathbf{H}\cdot\mathbf{g}\cdot\mathbf{S} + \mathbf{I}\cdot\mathbf{A}\cdot\mathbf{S} + P_{zz}[3I_z^2 - I(I+1)] + P_{xy}(I_x^2 - I_y^2) - g_n\beta_n\mathbf{H}\cdot\mathbf{I} \quad (1)$$

with $S = {}^1/_2$ and $I = {}^3/_2$. In eq 1 β and β_n are the Bohr magneton and nuclear magneton respectively, **g** is the electron **g** tensor, with the elements g_{ij} $(i, j = x, y, z)$, and **A** is the hyperfine tensor of ^{197}Au. $P_{ii} = |e|Qq_{ii}/4I(2I-1)$, where e is the electron charge, Q is the quadrupole moment of the nucleus, and $q_{ii} = \partial^2 V/\partial i^2$, the i component of the electric field gradient at the nucleus. $P_{xy} \equiv P_{xx} - P_{yy}$.

The general features of the principal axis spectra ($\mathbf{H} \| x, y, z$) are readily obtained from the solution of eq 1 by perturbation theory. Assuming that the principal axes systems of **g** and **A** coincide with **P** and neglecting off-diagonal elements of $\mathbf{I}\cdot\mathbf{A}\cdot\mathbf{S}$, we find that four "allowed" transitions and four weaker "forbidden" transitions are predicted. This result was also found by van Willigen and van Rens[15] in the absence of the nuclear Zeeman term. An interesting feature is that the weak satellites would become the allowed hyperfine lines if the quadrupole interaction were very small. This is graphically shown by Ranon and Stamirez,[16] who considered the case of $\mathbf{P} >> \mathbf{A}$. In the absence of the nuclear Zeeman interaction, pairs of "allowed" lines and pairs of "forbidden" lines may be picked out whose splittings are A_{ii} with $\mathbf{H} \| \mathbf{i}$. The effect of the nuclear Zeeman term is to cause the splittings between these pairs of lines to deviate from A_{ii} in a way which allows the determination of the absolute sign of the product $(A_{ii})(P_{ii})(g_n)$. However, this perturbation treatment is valid only at an extremely high microwave frequency (high field) since the neglected off-diagonal elements of $\mathbf{I}\cdot\mathbf{A}\cdot\mathbf{S}$ also

(15) H. van Willigen and J. G. M. van Rens, Quarterly Report, Vol. 2, Werkgroop voor Spectrochemie, Laboratorium voor Physische Chemie, Universiteit van Nijmegen, 1968.

(16) A. Ranon and D. N. Stamires, *Chem. Phys. Lett.*, 5, 221 (1970).

lead to unequal splittings of the pairs of lines. Abragam and Bleaney[17] have indicated how second-order terms in a spin Hamiltonian (eq 1) can allow the absolute determination of the signs of the spin-Hamiltonian parameters for the case of $A >> P$.

In order to be able to predict line positions and intensities accurately, with **H** in intermediate orientations, as well as along principal axes, a computer program[18] was written to diagonalize eq 1 with **H** referred to the principal axes system of **P**. In order to allow for the possible noncoincidence of principal axes systems, the program includes a provision for the independent rotation of **g** and **A** relative to **P**. The program is written for $S = 1/2$ and accepts $I \leq 9/2$. The output is either a printed stick spectrum or a plotted spectrum of gaussian or lorentzian lines of desired width and calculated intensity. The dashed curves of Figure 3 were calculated using the fitted values of the spin-hamiltonian parameters. The parameters of the spin Hamiltonian of $Au(mnt)_2^{2-}$ which best fit the observed spectra at 22 and $\sim -150°$ are given in Table I for the host crystals $Ni(mnt)_2(tba)_2 \cdot 2CH_3CN$ and $Ni(mnt)_2(tba)_2$. A plot of the temperature dependence of the principal values of **g** is given in Figure 4 and of the principal values of **A** and A_{iso} in Figure 5. There is very little anisotropy in **A**, and its principal directions were assumed to coincide with those of **P** since it was found that small rotations of **A** were experimentally undetectable. It is apparent that the sign of each principal value of **A** must be the same by comparison with the solution value, $a \cong A_{iso} = (A_{xx} + A_{yy} + A_{zz})/3$. The principal axes of **g** were found to coincide with those of **P** within experimental error[19] in the host $Ni(mnt)_2(tba)_2 \cdot 2CH_3CN$, as well as with the principal **g** axes of $Rh(mnt)_2^{2-}$ and $Cu(mnt)_2^{2-}$ which were present in small concentration in the crystal. In contrast, the principal **g** axes were found to be rotated relative to those of **P** in the hosts $M(mnt)_2(tba)_2$ (M = Ni, Pd, Pt). The principal axes of **P**, as well as the principal **g** axes of $Rh(mnt)_2^{2-}$ and $Cu(mnt)_2^{2-}$ present in the crystals, were found to coincide with the molecular axes of $M(mnt)_2^{2-}$. The absolute sense of the **g**-tensor rotation was determined from crystals which were oriented according to the known structure of the isomorphous M = Co complex.[13,20]

The effect of the misalignment of **g** relative to **P** is graphically illustrated in Figure 6, which gives the calculated and measured line positions and intensities for a crystal rotation with **H** in the *zx* molecular plane. The orientations at which the strong lines (and weak B lines) collapse are relatively insensitive to the orientation of **g**. Thus, they are observed to collapse at $\theta = -51.6°, +52.3°$ (±52°, within experimental error). The *g* value, however, is quite different for these orientations: $g(+52°) = 1.9979, g(-52°) = 1.9871$. These *g* values would be equal if the g axes system coincided with that of **P**. This is illustrated again in Figure 7 which shows the collapsed-orientation spectra for **H** in the *zx* and *zy* planes. The displacement of the spectrum of $Au(mnt)_2^{2-}$ relative to that of DPPH and $Cu(mnt)_2^{2-}$ is clearly evident in the *zx* spectra, but less so in the *zy* spectra. The rotation angle of **g** about *y* for the various hosts at room temperature, as well as the rotation angle in the M = Pt host at various temperatures, is given in Table II. It is noteworthy that the rotation angle is independent of the host metal, whereas the angle increases with decreasing temperature. The orientation of **g** relative to **P** (which is coincident with the molecular axes) is given in Figure 8 for the M = Ni host at 22°.[21] The

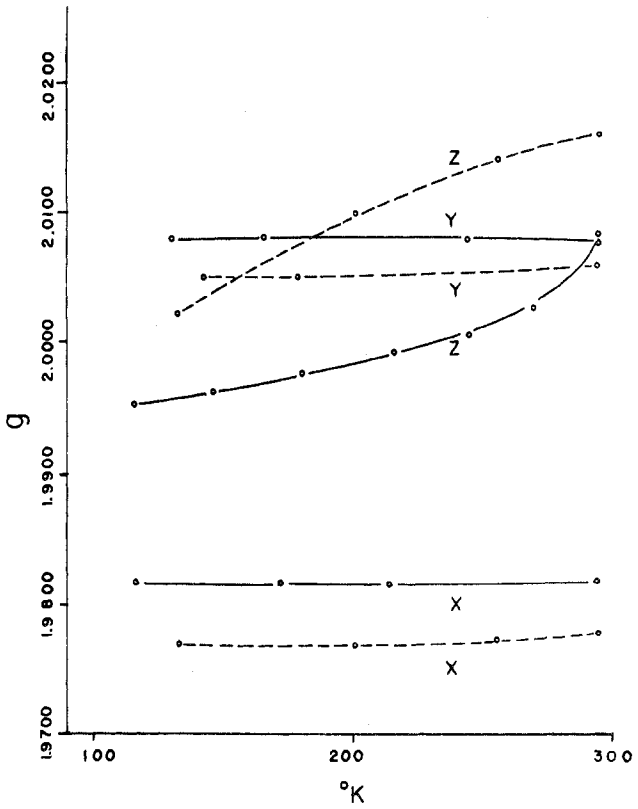

Figure 4. Temperature dependence of the principal *g* values of $Au(mnt)_2^{2-}$ in the host crystals $Ni(mnt)_2(tba)_2 \cdot 2CH_3CN$ (solid lines) and $Ni(mnt)_2(tba)_2$ (dashed lines).

Table I. Magnetic Parameters for $Au(mnt)_2^{2-}$ Doped into $Ni(mnt)_2(tba)_2$ and $Ni(mnt)_2(tba)_2 \cdot 2CH_3CN$

	$Ni(mnt)_2(tba)_2$[c,e]		$Ni(mnt)_2(tba)_2 \cdot 2CH_3CN$[d,e]	
	22°	−140°	22°	−150°
g_{xx}[a]	1.9777	1.9769	1.9819	1.9804
g_{yy}	2.0059	2.0051	2.0077	2.0080
g_{zz}	2.0160	2.0023	2.0084	1.9944
A_{xx}[b]	±39.2 ± 0.2	±43.9 ± 0.1	±40.0 ± 0.2	±43.9 ± 0.1
A_{yy}	±40.7 ± 0.2	±45.6 ± 0.1	±41.4 ± 0.2	±44.7 ± 0.1
A_{zz}	±41.5 ± 0.2	±46.6 ± 0.1	±42.4 ± 0.2	±47.1 ± 0.1
P_{zz}[b]	∓13.1 ± 0.1	∓13.98 ± 0.05	∓12.45 ± 0.1	∓13.00 ± 0.03
P_{xy}	±5.7 ± 0.1	±5.4 ± 0.2	±5.8 ± 0.1	±5.67 ± 0.03

$g_n(Au^{197}) = +0.0959 \pm 0.0003$[f]

[a] ±0.0003. [b] Units of 10^{-4} cm^{-1}. [c] The **g** tensor is found to be noncoincident with the molecular axes. The relationship between them at 22° is given in ref 21 and Figure 8. [d] The **g** tensor is found to be coincident with the molecular axes. [e] The **P** tensor is found to be coincident with the molecular axes while the **A** tensor is assumed to be coincident with the molecular axes. [f] From ref 22.

(17) A. Abragam and B. Bleaney, "Electron Paramagnetic Resonance of Transition Ions," Clarendon Press, Oxford, 1970, p 185.

(18) A complete listing of this Fortran IV program is given in the Ph.D. thesis of R. Schlupp, University of California, Riverside, Calif., 1973.

(19) The experimental error was ±2° except for rotation in the *yz* molecular plane which was several times larger due to the near equality of g_{yy} and g_{zz}.

(20) Unit cell parameters determined in this work for $M(mnt)_2(tba)_2$ are *b* (Å), a^* (Å^{-1}), c^* (Å^{-1}), β^* (deg) (M): 12.40, 0.1020, 0.1116, 65.3 (Ni); 12.48, 0.1024, 0.1118, 66.0 (Pd); 12.46, 0.1021, 0.1115, 64.8 (Pt); 12.35, 0.1024, 0.1123, 65.2 (Co).[13]

(21) The relationship at 22° between the **g** tensor in the molecular axis system, $\mathbf{g}_m$, and that in the principal axis system, $\mathbf{g}_d$, is given by the transformation $\mathbf{g}_m = \mathbf{T}^{tr} \cdot \mathbf{g}_d^2 \cdot \mathbf{T}$, where **T** is found to be

$$\mathbf{T} = \begin{pmatrix} 0.9883 & -0.0386 & 0.1478 \\ 0.0519 & 0.9949 & -0.0872 \\ -0.1437 & 0.0939 & 0.9852 \end{pmatrix}$$

Table II. $Au(mnt)_2^{2-}$ Epr Results for Rotation about the *y* Molecular Axis, in $M(mnt)_2(tba)_2$ Host[a,b]

	θ	g_{max}	g_{min}	A_{zz}	A_{xx}	P_{zz}	P_{xy}
Ni(22°)	8.5 ± 0.5	2.0162	1.9778	±41.3	±39.2	∓13.1	±5.8
Pd(22°)	8.5 ± 0.5	2.0164	1.9777	±41.1	±38.9	∓13.0	±5.8
Pt(22°)	8.5 ± 0.5	2.0164	1.9778	±41.4	±39.0	∓13.1	±5.8

	Pt(21°)	Pt(−17°)	Pt(−72°)	Pt(−140°)
θ	8.0	10.0	11.7	12.3
g_{max}	2.0160	2.0141	2.0100	2.0023
g_{min}	1.9777	1.9773	1.9768	1.9769
A_{iso}[c]	40.4	41.8	43.6	45.6

[a] *A* and *P* are in units of 10^{-4} cm^{-1}. The error limits are the same as in Table I. [b] g_{max}, g_{min}, and θ are from a least-squares analysis of the rotation data. θ (in degrees) is defined as the angle from g_{max} to the *z* molecular axis defined in Figure 8. [c] Ni host.

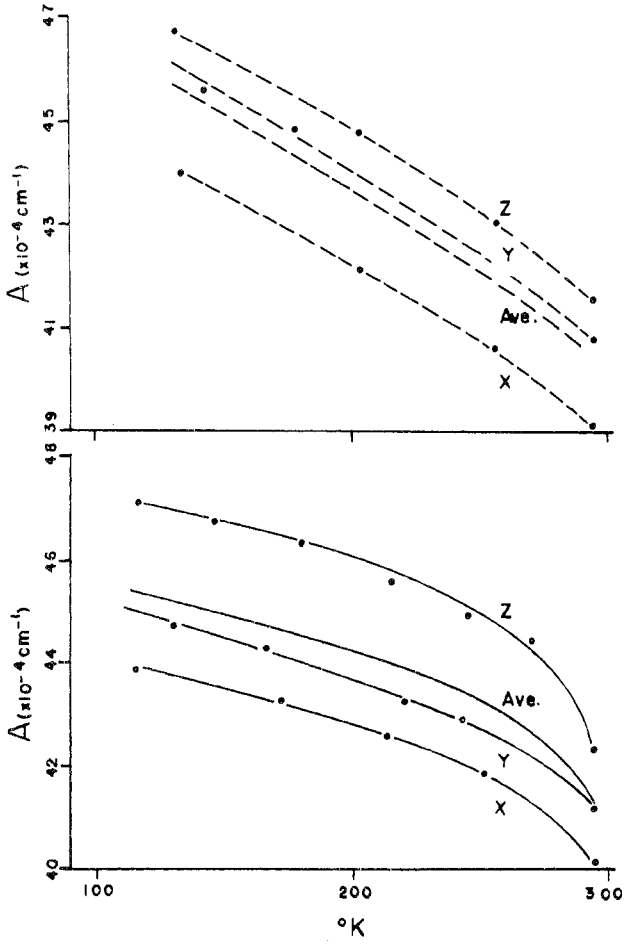

Figure 5. Temperature dependence of the principal ^{197}Au hyperfine constants and their average value A_{iso} for $Au(mnt)_2^{2-}$ in the host crystals $Ni(mnt)_2(tba)_2 \cdot 2CH_3CN$ (solid lines) and $Ni(mnt)_2(tba)_2$ (dashed lines).

z axis of g is directed nearly along the vector which connects Au with the nitrogen atoms of the neighboring tba^+ counterions.

As we noted above, the spacings between pairs of "allowed" and "forbidden" epr lines in the principal axis spectra differ from the principal value of the hyperfine tensor because of the effects of both the diagonal nuclear Zeeman term and the off-diagonal hyperfine interaction terms. These asymmetries could be accurately measured in the principal axis spectra of both hosts at ~−150° due to a considerable narrowing of the line widths as the temperature was decreased. The asymmetries were also calculated by the diagonalization of (1) for all possible values of the signs of A_{iso}, P_{zz}, and g_n.

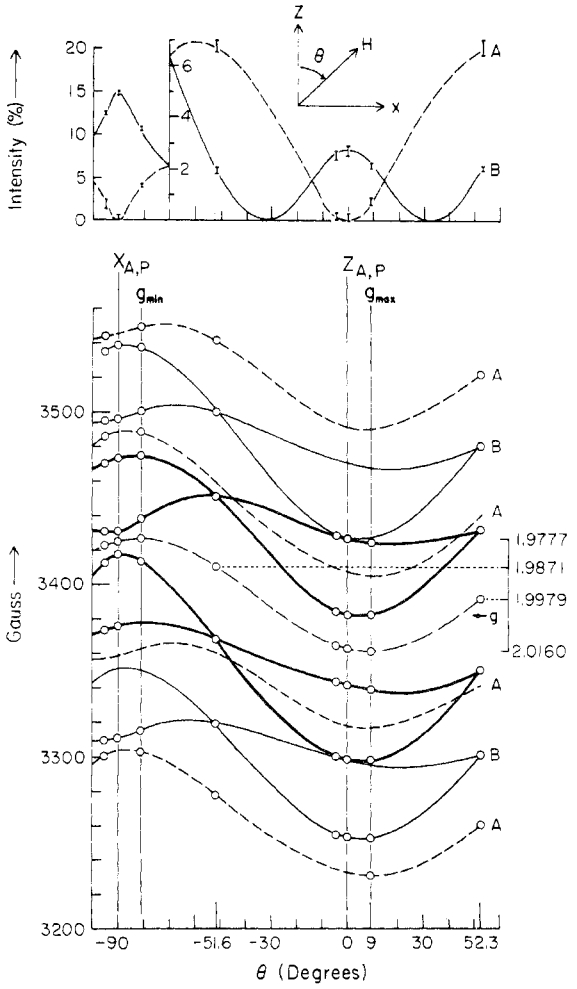

Figure 6. Comparison of the experimental and calculated epr line positions of $Au(mnt)_2^{2-}$ in a single crystal of $Ni(mnt)_2(tba)_2$ for a rotation with **H** in the *xz* molecular plane, at 22°. The "allowed" transitions are indicated by the heavier lines, while A and B label the two sets of "forbidden" lines. Intensities of the "forbidden" lines are given as percentages of the intensity of an "allowed" line. Microwave frequency is 9.4850 GHz.

The results of these calculations and the data for the $Ni(mnt)_2(tba)_2 \cdot 2CH_3CN$ host are presented in Table III. Only one set of predicted spacings is consistent with the measured spacings within experimental error, *e.g.*, $(A_{iso})(P_{zz})(g_n) = (+)(-)(+)$ or $(-)(+)(+)$. In order to be certain that the computer diagonalization of (1) was performed properly, the calculation of the principal-axis line spacings was repeated for a microwave frequency of 233 GHz. At this frequency, the second-order hyperfine contributions to the line shifts are completely negligible. The calculated line spacings then fall into just two sets, depending only upon the sign of the product $(A_{iso})(P_{zz})(g_n)$, in agreement with the perturbation theory calculation mentioned earlier. Thus, for $\mathbf{P} \cong \mathbf{A}$ it is apparently possible to determine the absolute sign of g_n when the nuclear Zeeman and second-order hyperfine contributions to the line shifts are comparable. This is seen to be positive for ^{197}Au.[22] It is also found that A_{iso} and P_{zz} have opposite signs. Since P_{zz} is most probably negative from theoretical considerations (*vide infra*), A_{iso} is predicted to be positive.

(22) H. H. Woodbury and G. W. Ludwig, *Phys. Rev.*, 117, 1287 (1960); E. Recknagel, *Z. Phys.*, 159, 19 (1960), also determined that the sign of g_n is positive from atomic beam measurements on Au-($^2S_{1/2}$).

Table III. Asymmetry in the X-Band Principal Axis Spectra of $Au(mnt)_2^{2-}$ Doped into $Ni(mnt)_2(tba)_2 \cdot 2CH_2CN$

Measd[a]			Calcd[b]										
				$A_{iso} \cdot P_{zz} \cdot g_n < 0$					$A_{iso} \cdot P_{zz} \cdot g_n > 0$				
Axis	$\Delta\Delta S$[c]	$\Delta\Delta W$[c]	Axis	A_{iso}	P_{zz}	g_n	$\Delta\Delta S$	$\Delta\Delta W$	A_{iso}	P_{zz}	g_n	$\Delta\Delta S$	$\Delta\Delta W$
x	1.86 ± 0.4	1.45 ± 0.4	x	+	−	+	1.66	1.66	+	−	−	1.21	0.94
y	1.7 ± 0.4	0.9 ± 0.4	y		or		1.44	1.09		or		0.83	0.84
z	1.4 ± 0.4	−1.7 ± 0.4	z	−	+	+	1.14	−1.80	−	+	−	1.24	−0.59
			x	+	+	−	0.0	0.64	+	+	+	0.20	−0.71
			y		or		0.53	0.03		or		−0.57	0.28
			z	−	−	−	0.8	1.35	−	−	−	1.45	2.01

[a] Temperature −150°. [b] The magnitudes of **g**, **A**, **P**, and g_n were taken from Table I. [c] $\Delta\Delta S = \Delta S_2 - \Delta S_1$ where the ΔS_i are in units of gauss and are the strong line separations which are approximately equal to the hyperfine splitting. The field increases from ΔS_1 to ΔS_2. $\Delta\Delta W$ is similarly defined for the weak lines.

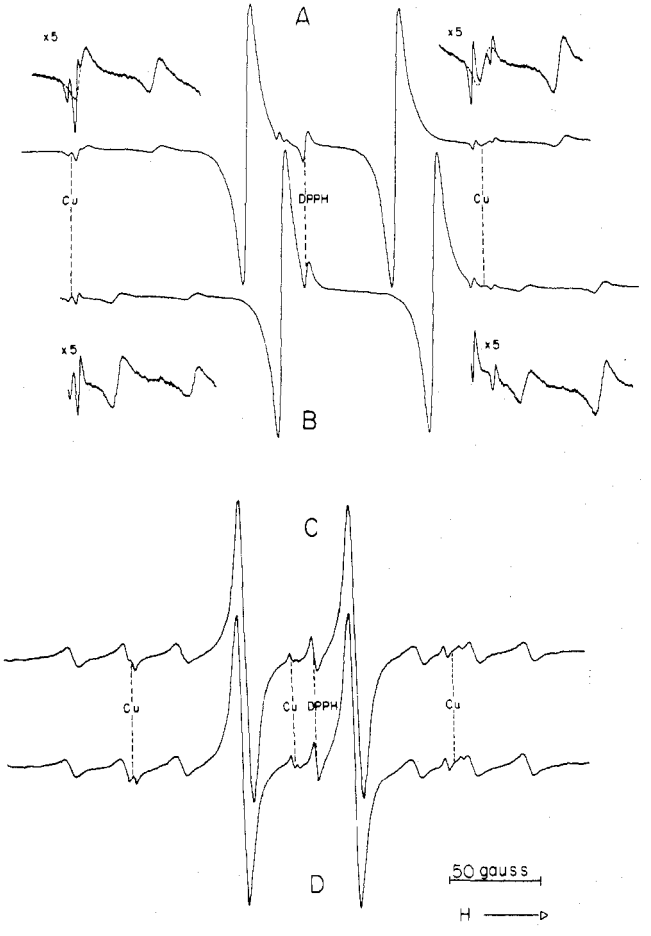

Figure 7. Epr spectra (22°) of $Au(mnt)_2^{2-}$ in $Ni(mnt)_2(tba)_2$ recorded with **H** along the directions of coalescence of the principal ^{197}Au hyperfine pattern in the xz and yz molecular planes. Polar angles (θ, ϕ) are **A** (52.3°, 0.0°), **B** (51.6°, 180.0°), **C** (62.9°, 90.0°), and **D** (63.2°, 270°).

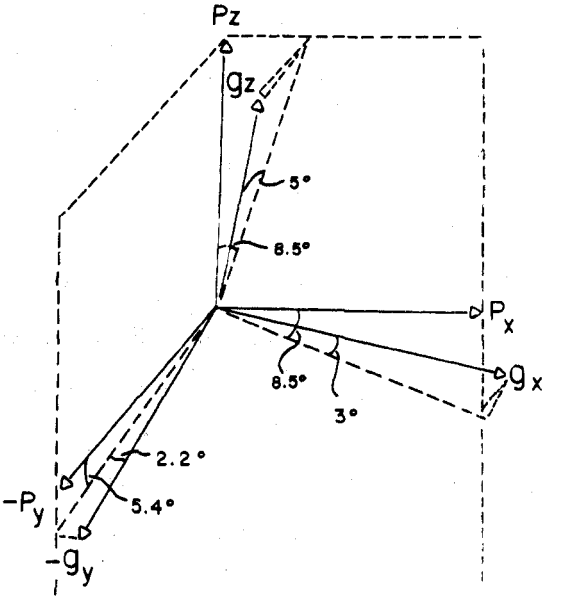

Figure 8. Orientation of the g tensor principal axes system relative to the quadrupolar axes system (coincident with the molecular axes) of $Au(mnt)_2^{2-}$ in $Ni(mnt)_2(tba)_2$ at 22°.

Discussion

The complex $Au(mnt)_2^{2-}$ is formally d^9 and in a square-planar ligand field would be expected to be analogous to Cu(II). It is well established that the spin hamiltonian of square-planar Cu(II) complexes can be explained by a ground-state electronic configuration containing a half-filled orbital of B_{1g} symmetry (a d_{xy} antibonding orbital in the coordinate system of Figure 1) which is generally partially delocalized over the ligand atoms.[23] Examination of the hyperfine tensor of ^{197}Au in $Au(mnt)_2^{2-}$ shows that it is unlikely that the half-filled orbital in the vicinity of the Au atom has much d character. The large isotropic component of A is most probably due to direct involvement of metal s character in the half-filled orbital. We can get a rough estimate of the coefficients of Au 6s and 5d contributions to the hyperfine tensor from calculations based on a localized electron spin in these metal orbital types. The 6s contribution to A_{iso} is given by

$$A_{iso} = A(6s) \cdot C_{6s}^2 \quad (2)$$

where C_{6s}^2 is the square of the coefficient of Ψ_{6s} in the half-filled orbital and

$$A(6s) = 8\pi g \cdot g_n \beta\beta_n |\Psi_{6s}(0)|^2/3hc \text{ cm}^{-1} \quad (3)$$

Similarly, the 5d contribution to the anisotropic part of A is given by

$$b = b(5d) \cdot C_{5d}^2 \quad (4)$$

where C_{5d}^2 is the contribution of Ψ_{5d} to the half-filled orbital and

$$b(5d) = 2g \cdot g_n \beta\beta_n \langle r^{-3} \rangle_{5d}/7hc \text{ cm}^{-1} \quad (5)$$

The principal values of the anisotropic contribution to A are given by $\pm b$, $\pm b$, and $\mp 2b$. Values for $|\Psi_{6s}(0)|^2$ and $\langle r^{-3} \rangle_{5d}$ obtained from the Hartree-Fock calculations of Fischer[24] are 11.36 and 13.33 au, respectively. Using $g_n = 0.0959$,[22]

(23) B. R. McGarvey, *J. Phys. Chem.*, 60, 71 (1956); A. H. Maki and B. R. McGarvey, *J. Chem. Phys.*, 29, 31 (1958).

(24) Supplement to C. Froese, *J. Chem. Phys.*, 45, 1417 (1966).

the calculated values of $A(6s)$ and $b(5d)$ are 291×10^{-4} and 11.6×10^{-4} cm^{-1}, respectively. Introducing the experimental values of $A_{iso} = 41 \times 10^{-4}$ cm^{-1} and $b \lesssim 1 \times 10^{-4}$ cm^{-1}, we find that $C_{6s}^2 = 0.14$ and $C_{5d}^2 \lesssim 0.09$.

There are two principal mechanisms which can provide s-orbital density in the unpaired electron wave function. The first is the direct admixture of the s orbital into the half-filled orbital, which requires that the orbital symmetry be A_g. The second is admixture through a spin-polarization mechanism,[25] which in this case might admix configurations such as (5s)-(5d)(6$\bar{s}$) with the configuration (5s)^2(5d). This mechanism places no restrictions on the 5d orbital symmetry. To estimate the magnitude of s-orbital density expected from the spin-polarization mechanism, we examined the magnetic parameters of $Cu(mnt)_2^{2-}$ [12] and $Pt(mnt)_2^-$.[26]

There is little likelihood that the ground-state wavefunction is totally symmetric in either of these complexes. Thus, the s admixture should come from the spin-polarization mechanism. Using values for $|\Psi_{ns}(0)|^2$ and $\langle r^{-3}\rangle_{nd}$ calculated from the tables of Fisher[24] for Cu(^{2}D), and Pt(^{3}F) and the experimental **A** tensors[12,26] we calculate that the s-orbital density induced by spin polarization is only 10–20% of the d-orbital density. We conclude that it is highly unlikely that the isotropic hyperfine contribution in $Au(mnt)_2^{2-}$ arises from a spin-polarization mechanism. It is more likely the result of direct admixture of Au 6s orbital into a half-filled orbital of A_g symmetry. The magnitude of the estimated 6s and 5d metal atom coefficients suggest that the half-filled orbital is predominantly ligand in character. We suppose that the B_{1g}* antibonding orbital which is half-filled in the Cu(II) analog lies above a predominantly ligand A_g orbital because of a general upward shift in the d atomic orbital energies associated with the heavier transition metals, an increase in the strength of the in-plane bonding, or a combination of both effects.

The isolated complex itself has D_{2h} point group symmetry which in the A_g irreducible representation allows mixing of metal 6s, $5d_{x^2-y^2}$, and $5d_{z^2}$ orbitals. The deviation of the principal g values from that of the free electron could then result from spin–orbit mixing with excited configurations of B_{1g}, B_{2g}, and B_{3g} orbital symmetry. The spin–orbit mixing is possible only if the A_g state has d-orbital character, provided spin–orbit coupling due to the sulfur nuclei is negligible relative to Au. However, a spin–orbit mechanism for the isolated complex $Au(mnt)_2^{2-}$ would leave the principal **g** axes coincident with the molecular symmetry axes and would not provide an explanation for the observed rotation of **g** relative to the molecular axes, its temperature dependence, or the temperature dependence of the principal values of **g** (primarily g_{zz}). The rotation of **g** relative to the molecular axes is most apparent in the isomorphous host crystals $M(mnt)_2(tba)_2$ (M = Ni, Pd, Pt), the structures of which are known,[13,20] and an explanation must be sought in the effects of the crystalline fields at the site of $Au(mnt)_2^{2-}$. The site symmetry at the gold atom is C_i, a point group which contains only the representations A_g and A_u. Thus, there are no restrictions on the mixing of d orbitals with an s orbital since all five d orbitals transform as A_g. Actually, the principal features of the rotation of **g** can be treated by the assumption that the effective site symmetry is C_{2h}, where the molecular y axis is taken as the C_2 axis. Under this C_{2h} point group, 6s, $5d_{z^2}$, $5d_{x^2-y^2}$, and $5d_{xz}$ transform as A_g, whereas $5d_{xy}$ and $5d_{yz}$ transform as B_g. Taking C_{2h} as the effective site symmetry seems reasonable since the positively charged N atoms of the tba^+ counterions, which probably exert the largest crystal field perturbation on the $Au(mnt)_2^{2-}$ ion, are located close to the xz plane of the complex and are displaced about 9° from the z axis defined in Figure 1. The effect of low-symmetry-induced mixing of $5d_{xz}$ into the half-filled orbital is to produce a rotation of **g** about y. The maximum electron density lobe is rotated in the xz plane, as well. A mechanism like the one envisioned here has been proposed by Hitchman, *et al.*,[27] to explain the in-plane g anisotropy of planar d^9 complexes of Cu(II), as well as the orientation of g_{max} and g_{min} in the molecular plane. Their theory can be extended in principle to the rotation of the **g** tensor in any plane, although it is cumbersome to apply to multielectron (or hole) configurations. In $Au(mnt)_2^{2-}$, we propose that the ground-state configuration is properly treated as a three-hole configuration $(B_g')^2(A_g')$ where B_g' is the antibonding orbital, B_{1g}*, in D_{2h} symmetry, which is half-occupied in square-planar Cu(II) complexes. The metal component of this orbital is d_{xy} in the coordinate system of Figure 1.

Although the low-symmetry-induced mixing of $5d_{xz}$ character into the half-filled A_g' orbital can account for the rotation of **g** in the xz plane, it is difficult to rationalize the large temperature dependence of the rotation angle (Table II) and of g_{zz} (Figure 4) on this basis alone. If a "normal" type d^9 configuration, $(B_g')(A_g')^2$, was the basis for a relatively low-lying excited electronic state, a thermally activated vibronic mechanism could be responsible for the temperature dependence of **g**. Specifically, low-lying vibrationally excited states of the lowest energy electronic configuration might be populated at elevated temperatures, and among these, those of B_g vibronic symmetry would be coupled with the electronic configuration $(B_g')(A_g')^2$. Finally, spin–orbit mixing of this configuration with excited d-orbital configurations would contribute to g shifts of the type typically observed in planar Cu(II) complexes. The rotation of g_{zz} *toward* the molecular z axis, in the $M(mnt)_2(tba)_2$ host crystals, as well as the increase in its magnitude with increasing temperature in both types of host are qualitatively in agreement with this mechanism. If the B_g' orbital is about 50% $5d_{xy}$, a value which is typical for copper(II)–dithiolene complexes,[12] a relatively small admixture of the $(B_g')(A_g')^2$ configuration is required to cause noticeable effects on **g**, particularly on the g_{zz} component, which is observed to be most affected. This is due, of course, to the large spin–orbit coupling constant of Au (~5000 cm^{-1}). Another important feature of the epr spectra which supports a mechanism operating through vibrationally excited states is the increase with temperature of the line widths in the magnetically dilute host crystals. If vibrational relaxation is rapid relative to the Larmor frequency shifts among the vibrational levels, the thermal-average **g** will be observed, but this mechanism will also contribute to spin–lattice relaxation and therefore to a broadening of the epr lines at elevated temperatures. A reasonable promoting mode for the temperature-dependent g shift is the Raman-active b_{1g} stretching mode (in D_{2h} symmetry) of the AuS_4 fragment. A reasonable estimate is about 300 cm^{-1} for this vibration, based upon the assignments of metal–sulfur vibrations of 1,2-dithiolenes,[28] the normal-coordinate analysis of

(25) B. R. McGarvey, *J. Phys. Chem.*, 71, 51 (1967).
(26) R. Schlupp, Thesis, University of California, Riverside, Calif., 1973.
(27) M. A. Hitchman, C. D. Olson, and R. L. Belford, *J. Chem. Phys.*, 50, 1195 (1969).
(28) D. M. Adams and J. B. Cornell, *J. Chem. Soc. A*, 1299 (1968).

platinum(II) dithiocarbamate,[29] and Raman spectral assignments of platinum(II) bis(trithiocarbonate).[30] The thermal population of the first excited vibronic level should be reasonably high at temperatures near room temperature ($kT \approx 200$ cm^{-1}).

We feel that the same mechanisms are operative in the host crystal $Ni(mnt)_2(tba)_2 \cdot 2CH_3CN$, which shows a similar temperature dependence of g_{zz}, but whose g tensor remains aligned with the molecular axis system at all temperatures investigated within experimental error. Although we do not know the crystal structure of this host, it is reasonable to assume that the CH_3CN molecules may act as axial ligands. If this is so, the site symmetry at the gold is probably much nearer D_{2h} since these ligands would shield the complex from the close approach of the perturbing tba^+ ions. The mixing of $5d_{xz}$ into the A_g' orbital would be reduced leaving the principal axes of g more coincident with the molecular axes. The vibronic mechanism discussed above is still operative so that g_{zz}, in particular, is temperature dependent.

This discussion has been of a qualitative nature. A detailed quantitative calculation of the model discussed above was carried out for the spin-Hamiltonian parameters of both hosts measured at several temperatures,[26] but because of its lengthy nature, it will not be reported here. A reasonable fit of the magnitudes, orientations, and temperature dependences of g, A, and P was obtained for both hosts with an approximately quantitative fit being obtained for the $Ni(mnt)_2(tba)_2$ host.

The quadrupole tensor, P, is mainly determined by the $(B_g')^2$ portion of the hole configuration, since the A_g' orbital is found to be largely spherically symmetric (6s) in the vicinity of Au. A sample calculation of P_{zz} neglecting Sternheimer antishielding[31] was carried out for the hole configuration $(5d_{xy})^2$ using $Q = 0.56 \times 10^{-24}$ cm^{-2} [32] and $\langle r^{-3} \rangle_{5d} = 13.3$ au.[24] The calculation gives $P_{zz}(5d_{xy}^2) = -58.4 \times 10^{-4}$ cm^{-1} and indicates that the metal 5d character of the B_g' orbital is about 25% when this result is compared with the experimental value of $|P_{zz}| \approx 13 \times 10^{-4}$ cm^{-1}. Although the numerical result should not be taken too seriously (calculations of quadrupole coupling constants tend to underestimate the metal character of the molecular orbitals),[33] it is consistent with a delocalized B_g' orbital. It was determined previously that the sign of A_{iso} is opposite to that of P_{zz}, and we can now infer that it is positive. The positive sign of A_{iso} provides additional evidence that it results from the direct admixture of gold 6s character into the half-filled orbital, since McGarvey has predicted that the spin-polarization mechanism would result in a negative A_{iso} for the third-row transition series.[25]

Finally, the temperature dependences of A_{iso} and P_{zz} are in quantitative agreement with the postulated vibronic mixing of the $(B_g')(A_g')^2$ configuration. A_{iso} increases with decreasing temperature, and the magnitude of the change can be accounted for[26] by the renormalization of the 6s component of A_g' as the contribution of the excited configuration decreases. $|P_{zz}|$ also increases with decreasing temperature (Table I) since thermal admixture of the excited configuration decreases the magnitude of the axial field gradient. Again, the magnitude of the temperature dependence agrees[26] with the configurational mixing required to fit the temperture dependence of g.

Conclusion

The epr of the complex ion $Au(mnt)_2^{-2}$ has been measured in several host crystals over a range of temperature. The results are consistent with a ground-state hole configuration $(B_{1g})^2(A_g)$ in D_{2h} symmetry. The B_{1g} orbital is normally half-filled in square-planar d^9 complexes. The A_g orbital is primarily a ligand-based orbital whose principal metal component is 6s (~15%) with smaller admixtures of metal 5d components. Thus, this complex probably is better described as a gold(III) complex with a radical anion ligand. Possibly the inability of most ligands to form such a structure explains the rarity of formal gold(II) complexes.

The g-tensor axes are found to be rotated from the molecular axes in the isomorphous host crystals $M(mnt)_2(tba)_2$ (M = Ni, Pd, Pt), an effect which is explained by the reduction of the site symmetry to C_{2h} (y as twofold axis) due to the electrostatic perturbation of the tba^+ ions. This allows the admixture of $5d_{xz}$ into the A_g orbital causing a rotation of g about the molecular y axis. The temperature dependence of g_{zz} and of the rotation angle of g is postulated to be due to vibronic mixing of the excited configuration $(B_g)(A_g)^2$; this model also explains the temperature dependence of P and A_{iso}. It has been possible to determine that the absolute sign of g_n for ^{197}Au is positive and that P_{zz} and A_{iso} have opposite signs. The proposed configuration makes P_{zz} negative so it is concluded that A_{iso} is most likely positive, in agreement with a direct 6s hyperfine mechanism rather than spin polarization.

Acknowledgments. We are grateful for the support of this work by a research grant from the National Science Foundation as well as a predoctoral fellowship from the National Institutes of Health, U. S. Public Health Service, to R. L. S. We wish to thank Professor R. Wing for guidance in the X-ray measurements.

Registry No. $Au(mnt)_2^{2-}$, 14977-46-9; $Ni(mnt)_2(tba)_2$, 42401-86-5; $Pd(mnt)_2(tba)_2$, 18958-59-3; $Pt(mnt)_2(tba)_2$, 42401-87-6.

(29) K. Nakamoto, J. Fujita, R. A. Condrate, and Y. Morimoto, *J. Chem. Phys.*, 39, 423 (1963).
(30) J. M. Burke and J. P. Fackler, Jr., *Inorg. Chem.*, 11, 2744 (1972).
(31) R. M. Sternheimer, *Phys. Rev.*, 95, 736 (1954).
(32) G. H. Fuller and V. W. Cohen, *Nucl. Data, Sect. A*, 5, 433 (1969).
(33) H. So and R. L. Belford, *J. Amer. Chem. Soc.*, 91, 2392 (1969).